

# Towards Optimal Correlational Object Search

Kaiyu Zheng<sup>†</sup>, Rohan Chitnis<sup>\*</sup>, Yoonchang Sung<sup>\*</sup>, George Konidaris<sup>†</sup>, Stefanie Tellex<sup>†</sup>

**Abstract**—In realistic applications of object search, robots will need to locate target objects in complex environments while coping with unreliable sensors, especially for small or hard-to-detect objects. In such settings, *correlational information* can be valuable for planning efficiently: when looking for a fork, the robot could start by locating the easier-to-detect refrigerator, since forks would probably be found nearby. Previous approaches to object search with correlational information typically resort to ad-hoc or greedy search strategies. In this paper, we propose the Correlational Object Search POMDP (COS-POMDP), which can be solved to produce search strategies that use correlational information. COS-POMDPs contain a correlation-based observation model that allows us to avoid the exponential blow-up of maintaining a joint belief about all objects, while preserving the optimal solution to this naive, exponential POMDP formulation. We propose a hierarchical planning algorithm to scale up COS-POMDP for practical domains. We conduct experiments using AI2-THOR, a realistic simulator of household environments, as well as YOLOv5, a widely-used object detector. Our results show that, particularly for hard-to-detect objects, such as scrub brush and remote control, our method offers the most robust performance compared to baselines that ignore correlations as well as a greedy, next-best view approach.

## I. INTRODUCTION

Object search is a fundamental capability for robots in many applications including domestic services [1, 2], search and rescue [3, 4], and elderly care [5, 6]. In realistic settings, the object being searched for will often be small, outside the current field of view, and hard to detect. For example, a household robot must be very close to a fork in order to be able to detect it; likewise, a warehouse robot may have to locate a particular machine within a very large factory. To be effective, the robot must generate efficient search strategies that require as few timesteps as possible.

In such settings, when the target object is hard to detect, *correlational information* can be extremely useful. Specifically, suppose the robot is equipped with a prior about the relative spatial locations of object types (*e.g.*, refrigerators tend to be near forks). Then, it can leverage this information as a powerful heuristic to narrow down or “focus” the search space, by first focusing its efforts on locating easier-to-detect objects that are highly correlated with the target object, and only then focusing on locating the target object itself. Doing so has the potential to greatly improve search efficiency, as the robot no longer needs to waste time considering strategies that, *e.g.*, search for a fork in a bathroom. Unfortunately, previous approaches to object

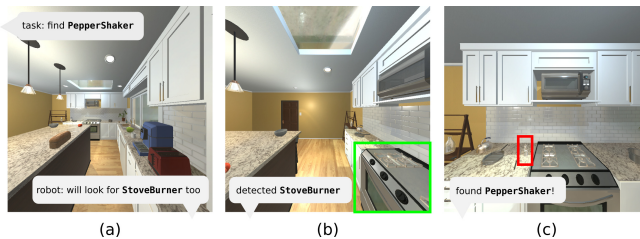


Fig. 1: We study the problem of object search using correlational information about spatial relations between objects. This example illustrates a desirable search behavior in an AI2-THOR scene, where the robot leverages the detection of a StoveBurner to more efficiently find a hard-to-detect PepperShaker.

search with correlational information tend to resort to ad-hoc or greedy search strategies [7, 8, 2], which may not scale well to complex environments.

We follow a long line of work that models the object search problem as a partially observable Markov decision process (POMDP) [7, 9, 10, 11, 12]. This formalization is useful because object search over long horizons is naturally a sequential, partially observed decision-making problem: (1) the robot must search for the target object by visiting multiple viewpoints in the environment sequentially, and (2) the robot must maintain and update a measure of uncertainty over the location of the target object, via its belief state.

In this paper, we propose a novel planning framework for optimal object search with given correlational information, COS-POMDP (Correlational Object Search POMDP). Critically, COS-POMDPs avoid the exponential blow-up of naively maintaining a joint belief about all objects. Instead, we derive a correlation-based observation model and prove that COS-POMDPs, which use this model, produce equivalent solutions to the exponential formulation. The correlational information is given to the robot as a factored joint distribution over object locations. In practice, this distribution can be approximated by learning it from data [8, 13] or interpreting human speech [14, 15].

We make the following contributions: (1) We propose COS-POMDP, which contains a correlation-based observation model that captures spatial relations between objects; (2) We prove that COS-POMDPs produce equivalent solutions to a naive formulation where the state space is a joint over all object locations, despite COS-POMDPs having a much smaller state space; (3) We address scalability by proposing a hierarchical planning algorithm, where a high-level COS-POMDP plans subgoals, each fulfilled by a low-level planner that plans with low-level actions (*i.e.*, given primitive actions); both levels plan online based on a shared and updated

<sup>†</sup>Brown University, Providence, RI. <sup>\*</sup>MIT CSAIL, Cambridge, MA.  
Email correspondence: {kzheng10@cs.brown.edu}

COS-POMDP belief state, enabling closed-loop planning; (4) We investigate the influence of correlational information when searching for hard-to-detect targets, and the benefit of optimizing for a sequence of actions as opposed to selecting the next-best view. We conduct experiments in AI2-THOR [16], a realistic simulator of household environments, and use YOLOv5 [17, 18] as the object detector. Our results show that, when the given correlational information is accurate, COS-POMDP leads to more robust search performance when the target object is hard to detect. In particular, for target objects with a true positive detection rate below 40%, COS-POMDP improves the POMDP baseline that ignores correlational information by 70% and a greedy, next-best view baseline by 170%, in terms of the SPL [19] metric, commonly used for evaluating navigation agents in simulated environments [20, 21, 22].

## II. RELATED WORK

Object search involves a wide range of subproblems (*e.g.*, perception [7, 10], planning [23, 9], manipulation [24, 25]) and different types of target objects (moving [26] or static [23]). The search environment could be unknown, requiring the robot to build a map during search [7, 27]; or the robot could be given a pre-built map for navigation [8, 28, 11] that may contain landmarks with partially or fully known locations [2, 29, 30]. We consider static objects and an environment where the set of possible object locations is given, but no object location is known a priori. Our approach allows information about landmark locations to be easily incorporated to reduce the robot’s initial uncertainty over the target object’s location.

Garvey [31] and Wixson and Ballard [32] pioneered the paradigm of *indirect search*, where an intermediate object (such as a desk) that is typically easier to detect is located first, before the target object (such as a keyboard). More recently, probabilistic graphical models have been used to model object-room or object-object spatial correlations [7, 2, 8, 28]. In particular, Zeng et al. [2] proposed a factor graph representation for different types of object spatial relations. Their approach produces search strategies in a greedy fashion by selecting the next-best view to navigate towards, based on a hybrid utility of navigation cost and the likelihood of detecting objects. In our evaluation, we compare our sequential decision-making approach with a greedy, next-best view baseline based on that work [2].

Recently, the problem of semantic visual navigation [33, 22, 20, 21, 34] received a surge of interest in the deep learning community. In this problem, an embodied agent is placed in an unknown environment and tasked to navigate towards a given semantic target (such as “kitchen” or “chair”). The agent typically has access to behavioral datasets for training on the order of millions of frames and the challenge is typically in generalization. Our work considers the standard evaluation metric (SPL [19]) and task success criteria (object visibility and distance threshold [22]) from this body of work. However, our setting differs fundamentally in that the

search strategy is not a result of training but a result of solving an optimization problem.

## III. PROBLEM FORMULATION

We formulate correlational object search as a planning problem, where a robot must search for a target object given correlational information with other objects in the environment. We begin by describing the underlying search environment and the capabilities of the robot. Then we define the inputs to the robot and the solution expected to be produced by the robot to solve this problem.

### A. Search Environment and Robot Capabilities

The search environment contains a target object and  $n$  additional static objects. The set of possible object locations is discrete, denoted as  $\mathcal{X}$ . The locations of the target object  $x_{\text{target}} \in \mathcal{X}$  and other objects  $x_1, \dots, x_n \in \mathcal{X}$  are unknown to the robot, and follow a latent joint distribution  $\Pr(x_1, \dots, x_n, x_{\text{target}})$ . The robot is given as input a factored form of this distribution, defined later in Sec. III-B.

The robot can observe the environment from a discrete set of viewpoints, where each viewpoint is specified by the position and orientation of the robot’s camera. These viewpoints form the necessary state space of the robot, denoted as  $\mathcal{S}_{\text{robot}}$ . The initial viewpoint is denoted as  $s_{\text{robot}}^{\text{init}}$ . By taking a primitive move action  $a$  from the set  $\mathcal{A}_m$ , the robot changes its viewpoint subject to transition uncertainty  $T_m(s'_{\text{robot}}, s_{\text{robot}}, a) = \Pr(s'_{\text{robot}} | s_{\text{robot}}, a)$ . Also, the robot can decide to finish a task at any timestep by choosing a special action Done, which deterministically terminates the process.

At each timestep, the robot receives an observation  $z$  factored into two independent components  $z = (z_{\text{robot}}, z_{\text{objects}})$ . The first component  $z_{\text{robot}} \in \mathcal{S}_{\text{robot}}$  is an estimation of the robot’s current viewpoint following the observation model  $O_{\text{robot}}(z_{\text{robot}}, s_{\text{robot}}) = \Pr(z_{\text{robot}} | s_{\text{robot}})$ . The second component  $z_{\text{objects}} = (z_1, \dots, z_n, z_{\text{target}})$  is the result of performing object detection. Each element,  $z_i \in \mathcal{X} \cup \{\text{null}\}$ ,  $i \in \{1, \dots, n, \text{target}\}$ , is the detected location of object  $i$  within the field of view, or null if not detected. The observation  $z_i$  about object  $i$  is subject to limited field of view and sensing uncertainty captured by a *detection model*  $D_i(z_i, x_i, s_{\text{robot}}) = \Pr(z_i | x_i, s_{\text{robot}})$ ; Here, a common conditional independence assumption in object search is made [2, 11], where  $z_i$  is conditionally independent of the observations and locations of all other objects given its location and the robot state  $s_{\text{robot}}$ . The set of detection models for all objects is  $\mathcal{D} = \{D_1, \dots, D_n, D_{\text{target}}\}$ . In our experiments, we obtain parameters for the detection models based on the performance of the vision-based object detector (Sec. VI-B).

### B. The Correlational Object Search Problem

Although the joint distribution of object locations is latent, the robot is assumed to have access to a factored form of that distribution, that is,  $n$  conditional distributions,  $\mathcal{C} = \{C_1, \dots, C_n\}$  where  $C_i(x_i, x_{\text{target}}) = \Pr(x_i | x_{\text{target}})$  specifies the spatial correlation between the target and object  $i$ . We call

each  $C_i$  a *correlation model*. This model can be learned from data or specified based on environment-specific knowledge.

The robot performs search by taking a sequence of move actions to observe different parts of the environment, and terminates the search by taking Done. We are now ready to define the *correlational object search* problem:

**Problem 1 (Correlational Object Search).** Given as input a tuple  $(\mathcal{X}, \mathcal{C}, \mathcal{D}, s_{\text{robot}}^{\text{init}}, \mathcal{S}_{\text{robot}}, \mathcal{O}_{\text{robot}}, \mathcal{A}_m, T_m)$ , the robot must perform a sequence of actions,  $a_{1:T} = (a_1, \dots, a_T)$  of length  $T \geq 1$ , where  $a_1, \dots, a_{T-1} \in \mathcal{A}_m$  and  $a_T$  is Done. The action sequence  $a_{1:T}$  is called a *solution*. A solution is *successful* if the robot state sequence and the target location satisfy certain criteria upon taking the Done action. In our evaluation in AI2-THOR, we use the success criteria recommended by Batra et al. [22] and the commonly-used SPL metric proposed by Anderson et al. [19] to measure the efficiency of successful searches. The objective is to produce a successful solution that reaches the target object while minimizing the total distance traveled by the robot.

#### IV. CORRELATIONAL OBJECT SEARCH AS A POMDP

The POMDP is an extensively studied framework for optimizing sequential decisions under partial observability and uncertainty in motion and sensing. Both challenges (partial observability and uncertainty) considered in POMDP arise naturally in object search. In addition, the objective of minimizing the navigation distance while successfully finding the target can be represented by the POMDP objective of maximizing the discounted cumulative rewards. Therefore, we model the correlational object search task as a POMDP.

We first provide a condensed review of POMDPs; for more information, we refer the reader to [35, 36, 37, 38]. Then, we present the COS-POMDP, a POMDP formulation that addresses the correlational object search problem, followed by a discussion on its optimality.

##### A. Background: POMDPs

Formally, a POMDP is a tuple  $(\mathcal{S}, \mathcal{A}, \mathcal{Z}, T, O, R, \gamma)$ , where  $\mathcal{S}, \mathcal{A}, \mathcal{Z}$  denote the state, action, and observation spaces,  $T(s', a, s) = \Pr(s'|s, a)$ ,  $O(z, s', a) = \Pr(z|s', a)$  are the transition and observation models, and  $R(s, a) \in \mathbb{R}$  is the reward function. At each timestep, the agent takes an action  $a \in \mathcal{A}$ , the environment state transitions from  $s \in \mathcal{S}$  to  $s' \in \mathcal{S}$  according to  $T$ , and the agent receives an observation  $z \in \mathcal{Z}$  from the environment according to  $O$ .

The agent typically maintains a *belief state*  $b_t : \mathcal{S} \rightarrow [0, 1]$ , a distribution over the states and a sufficient statistic for the history of past actions and observations  $h_t = (az)_{1:t-1}$ . The agent updates its belief after taking action  $a$  and receiving observation  $z$ :  $b^{z,a}(s') = \eta O(z, s', a) \sum_s T(s', a, s) b(s)$ , where  $\eta$  is the normalizing constant [35].

The solution to a POMDP is a *policy*  $\pi$  that maps a history to an action. The *value* of a POMDP at a history under policy  $\pi$  is the expected discounted cumulative reward following that policy:  $V_\pi(h) = \mathbb{E}[\sum_{t=0}^{\infty} \gamma^t R(s_t, \pi(h_t)) | h_0 = h]$  where  $\gamma$  is the discount factor. The optimal value at the history is  $V(h) = \max_\pi V_\pi(h)$ .

##### B. COS-POMDP

Given an instance of the correlational object search problem defined in Sec. III-B, we define the **Correlational Object Search POMDP (COS-POMDP)** as follows:

- **State space.** The state space  $\mathcal{S}$  is factored to include the robot state  $s_{\text{robot}} \in \mathcal{S}_{\text{robot}}$  and the target state  $x_{\text{target}} \in \mathcal{X}$ . A state  $s \in \mathcal{S}$  can be written as  $s = (s_{\text{robot}}, x_{\text{target}})$ . Importantly, no other object state is included in  $\mathcal{S}$ .
- **Action space.** The action space is  $\mathcal{A} = \mathcal{A}_m \cup \{\text{Done}\}$ .
- **Observation space.** The observation space  $\mathcal{Z}$  is factored over the objects, and each  $z \in \mathcal{Z}$  is written as  $z = (z_{\text{robot}}, z_{\text{objects}})$ , where  $z_{\text{objects}} = (z_1, \dots, z_n, z_{\text{target}})$ .
- **Transition model.** The objects are assumed to be static. Actions  $a_m \in \mathcal{A}_m$  change the robot state from  $s_{\text{robot}}$  to  $s'_{\text{robot}}$  according to  $T_m$ , and taking the Done action terminates the task deterministically.
- **Observation model.** By definition of  $z$ , we have

$$\Pr(z|s) = \Pr(z_{\text{robot}}|s_{\text{robot}}) \Pr(z_{\text{objects}}|s) \quad (1)$$

$$= O_{\text{robot}}(z_{\text{robot}}, s_{\text{robot}}) \Pr(z_{\text{objects}}|s) \quad (2)$$

Under the conditional independence assumption in Sec. III,  $\Pr(z_{\text{objects}}|s)$  can be compactly factored as:

$$\Pr(z_{\text{objects}}|s) = \Pr(z_1, \dots, z_n, z_{\text{target}}|x_{\text{target}}, s_{\text{robot}}) \quad (3)$$

$$= \Pr(z_{\text{target}}|x_{\text{target}}, s_{\text{robot}}) \prod_{i=1}^n \Pr(z_i|x_{\text{target}}, s_{\text{robot}}) \quad (4)$$

The first term in Eq (4) is defined by  $D_{\text{target}}$ , and each  $\Pr(z_i|x_{\text{target}}, s_{\text{robot}})$  is called a *correlational observation model*, written as:

$$\Pr(z_i|x_{\text{target}}, s_{\text{robot}}) = \sum_{x_i \in \mathcal{X}} \Pr(x_i, z_i|x_{\text{target}}, s_{\text{robot}}) \quad (5)$$

$$= \sum_{x_i \in \mathcal{X}} \Pr(z_i|x_i, s_{\text{robot}}) \Pr(x_i|x_{\text{target}}) \quad (6)$$

where the two terms in Eq (6) are the detection model  $D_i \in \mathcal{D}$  and correlation model  $C_i \in \mathcal{C}$ , respectively.

- **Reward function.** The reward function,  $R(s, a) = R(s_{\text{robot}}, x_{\text{target}}, a)$ , is defined as follows. Upon taking Done, the task outcome is determined based on  $s_{\text{robot}}, x_{\text{target}}$ , which is successful if the robot orientation is facing the target and its position is within a distance threshold to the target. If successful, then the robot receives  $R_{\text{max}} \gg 0$ , and  $R_{\text{min}} \ll 0$  otherwise. Taking a move action from  $\mathcal{A}_m$  receives a negative reward which corresponds to the action's cost. In our experiments, we set  $R_{\text{max}} = 100$  and  $R_{\text{min}} = -100$ . Each primitive move action (e.g., MoveAhead) receives a step cost of -1.

##### C. Optimality of COS-POMDPs

The state space of a COS-POMDP involves only the robot and target object states. A natural question arises: have we lost any necessary information? In this section, we show that COS-POMDPs are optimal, in the following sense. If we imagine solving a “full” POMDP corresponding to the COS-POMDP, whose state space contains all object states, then



the solutions to the COS-POMDP are equivalent. Note that a belief state in this “full” POMDP scales exponentially in the number of objects.

We begin by precisely defining the “full” POMDP, henceforth called the F-POMDP, corresponding to a COS-POMDP. The F-POMDP has identical action space, observation space, and transition model as the COS-POMDP. The reward function is also identical since it only depends on the target object state, robot state, and the action taken. F-POMDP differs in the state space and observation model:

- **State space:** The state is  $s = (s_{\text{robot}}, x_{\text{target}}, x_1, \dots, x_n)$ .
- **Observation model:** Under the conditional independence assumption stated in Sec. III, the model for observation  $z_i$  of object  $x_i$  involves just the detection model:  $\Pr(z_i|s) = \Pr(z_i|x_i, s_{\text{robot}})$ .

Since the COS-POMDP and the F-POMDP share the same action and observation spaces, they have the same history space as well. We first show that given the same policy, the two models have the same distribution over histories.

**Theorem 1.** Given any policy  $\pi : h_t \rightarrow a$ , the distribution of histories is identical between the COS-POMDP and the F-POMDP.

*Proof:* See Appendix A. ■

Using Theorem 1, we are equipped to make a statement about the value of following a given policy in either the COS-POMDP or the F-POMDP.

**Corollary 1.** Given any policy  $\pi : h_t \rightarrow a$  and  $h_t$ , the value  $V_\pi(h_t)$  is identical between the COS-POMDP and the F-POMDP.

*Proof:* By definition, the value of a POMDP at a history is the expected discounted cumulative reward with respect to the distribution of future action-observation pairs. Theorem 1 states that the COS-POMDP and F-POMDP have the same distribution of histories given  $\pi$ . Furthermore, the reward function depends only on the states of the robot and the target object. Thus, this expectation is equal for the two POMDPs at any  $h$ . ■

Finally, we can show that COS-POMDPs are optimal in the sense that we described before.

**Corollary 2.** An optimal policy  $\pi^*$  for either the COS-POMDP or the F-POMDP is also optimal for the other.

*Proof:* Suppose, without loss of generality, that  $\pi^*$  is optimal for the COS-POMDP but not the F-POMDP. Let  $\pi'$  be the optimal policy for the F-POMDP. By the definition of optimality, for at least some history  $h$  we must have  $V_{\pi'}(h) > V_{\pi^*}(h)$ . By Corollary 1, for any such  $h$  the COS-POMDP also has value  $V_{\pi'}(h)$ , meaning  $\pi^*$  is not actually optimal for the COS-POMDP; this is a contradiction. ■

## V. HIERARCHICAL PLANNING

Despite the optimality-preserving reduction of state space in a COS-POMDP, directly planning over the primitive move actions is not scalable to practical domains even for state-of-the-art online POMDP solvers [38]. This is especially the case when in-place rotation actions are considered, since identical viewpoints may be repeatedly visited at different depth levels in the search tree, limiting the size of the

---

### Algorithm 1: OnlineHierarchicalPlanning

---

**Input:**  $P = (\mathcal{X}, \mathcal{C}, \mathcal{D}, s_{\text{robot}}^{\text{init}}, \mathcal{S}_{\text{robot}}, \mathcal{O}_{\text{robot}}, \mathcal{A}_m, T_m)$ .

**Parameter:** maximum number of steps  $T_{\text{max}}$ .

**Output:** A solution  $a_{1:T}$  (Problem 1).

$b_{\text{target}}^1(x_{\text{target}}) \leftarrow \text{Uniform}(\mathcal{X})$ ;

$b_{\text{robot}}^1(s_{\text{robot}}) \leftarrow \mathbb{1}(s_{\text{robot}} = s_{\text{robot}}^{\text{init}})$ ;

$b^1 \leftarrow (b_{\text{target}}^1, b_{\text{robot}}^1)$ ;

$t \leftarrow 1$ ;

**while**  $t \leq T_{\text{max}}$  and  $a_{t-1} \neq \text{Done}$  **do**

$(\mathcal{V}, \mathcal{E}) \leftarrow \text{SampleTopoGraph}(\mathcal{X}, \mathcal{S}_{\text{robot}}, b_{\text{target}}^t)$ ;

$P_H \leftarrow \text{HighLevelCOSPOMDP}(P, \mathcal{V}, \mathcal{E}, b^t)$ ;

    subgoal  $\leftarrow$  plan POMDP online for  $P_H$ ;

**if** subgoal is *navigate to a node in*  $\mathcal{V}$  **then**

$s_{\text{robot}} \leftarrow \arg\max_{s_{\text{robot}}} b_{\text{robot}}(s_{\text{robot}})$ ;

$a_t \leftarrow A^*(\text{subgoal}, s_{\text{robot}}, \mathcal{A}_m, T_m)$ ;

**else if** subgoal is *search locally* **then**

$P_L \leftarrow \text{LowLevelCOSPOMDP}(P, b^t)$ ;

$a_t \leftarrow$  plan POMDP online for  $P_L$ ;

**else if** subgoal is *Done* **then**

$a_t \leftarrow \text{Done}$

**end**

$z_t \leftarrow$  execute  $a_t$  and receive observation;

$b^{t+1} \leftarrow \text{BeliefUpdate}(b^t, a_t, z_t)$ ;

$t \leftarrow t + 1$ ;

**end**

---

search region considered during planning. At the same time, however, planning POMDP actions at the low level has the benefit of controlling fine-grained movements, allowing goal-directed behavior to emerge automatically at this level. Therefore, we seek an algorithm that can reason about both searching over a large region as well as careful search in the area around the robot. This is practical because typical mobile robots can be controlled both at the low level of motor velocities and the high level of navigation goals [39, 40].

Hence, we propose a hierarchical planning algorithm to apply COS-POMDPs in realistic domains. The algorithm is presented in Algorithm 1 and illustrated in Fig 2. To enable the planning of searching over a large region, we first generate a topological graph, where nodes are places accessible by the robot, and edges indicate navigability between places [41]. This is done by the SampleTopoGraph procedure (Appendix B). In this procedure, the nodes are sampled based on the robot’s current belief in the target location  $b_{\text{target}}^t$ , and edges are added such that the graph is connected and every node has an out-degree within a given range, which affects the branching factor for planning. An example output is illustrated in Fig 2.

Then, a high-level COS-POMDP  $P_H$  is instantiated. The state and observation spaces, the observation model, and the reward model, are as defined in Sec IV-B. The move action set and the corresponding transition model are defined according to the generated topological graph. Each move action represents a subgoal of *navigating* to another place, or the subgoal of *searching locally* at the current place.

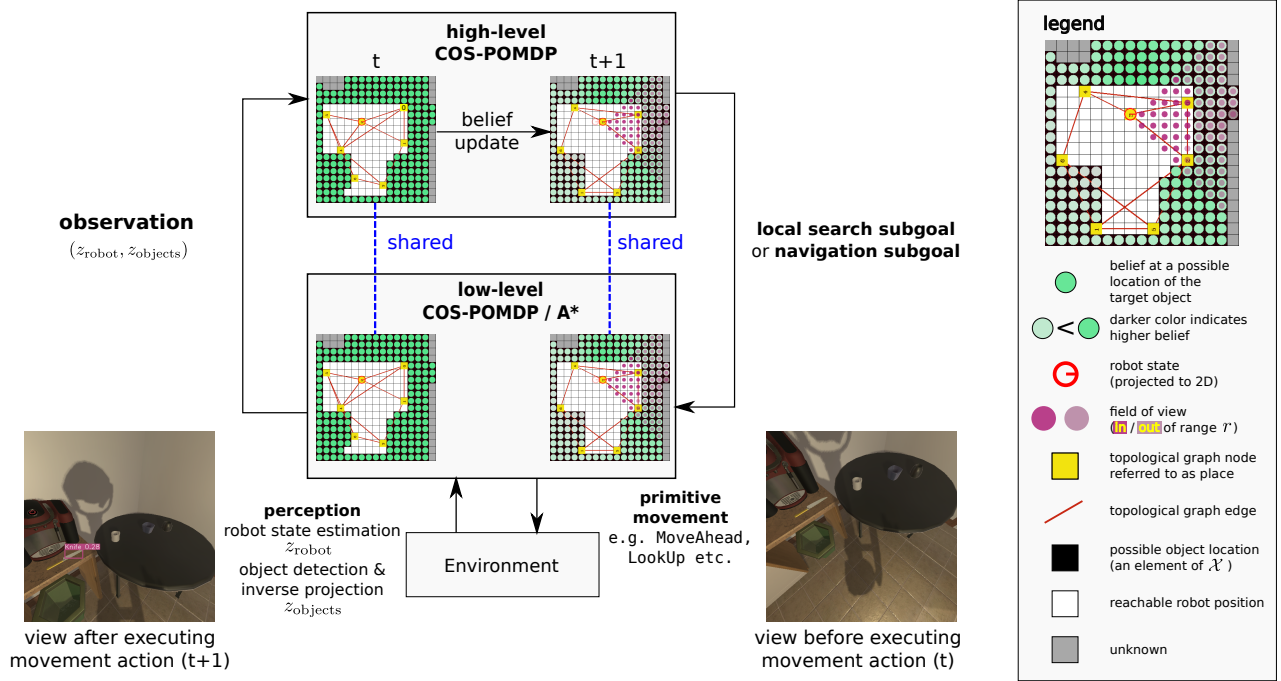


Fig. 2: **Illustration of the Hierarchical Planning Algorithm.** A high-level COS-POMDP plans subgoals that are fed to a low-level planner to produce low-level actions. The belief state is shared across the levels. Both levels plan with updated beliefs at every timestep.

Both types of subgoals can still be understood as viewpoint-changing actions, except the latter keeps the viewpoint at the same location. For the transition model  $T(s', g, s)$  where  $g$  represents the subgoal, the resulting viewpoint (i.e.,  $s'_{\text{robot}} \in s'$ ) after completing a subgoal is located at the destination of the subgoal with orientation facing the target object location ( $x_{\text{target}} \in s$ ). The Done action is also included as a dummy subgoal to match the definition of the COS-POMDP action space (Sec IV-B).

At each timestep, a subgoal is planned using an online POMDP planner, and a low-level planner is instantiated corresponding to the subgoal. This low-level planner then plans to output an action  $a_t$  from the action set  $\mathcal{A} = \mathcal{A}_m \cup \{\text{Done}\}$ , which is used for execution. In our implementation, for *navigation* subgoals, an A\* planner is used, and for *searching locally*, a low-level COS-POMDP  $P_L$  is instantiated with the primitive movements  $\mathcal{A}_m$  in its action space. (We use POUCT [38] as the online POMDP solver in our experiments.)

Upon executing the low-level action  $a_t$ , the robot receives an observation  $z_t \in \mathcal{Z}$  from its on-board perception modules for robot state estimation and object detection. This observation is used to update the belief of the high-level COS-POMDP, which is shared with the low-level COS-POMDP.

Finally, the process starts over from the first step of sampling a topological graph. If the high-level COS-POMDP plans a new subgoal different the current one, then the low-level planner is re-instantiated.

This algorithm plans actions for execution in an online, closed-loop fashion, allowing reasoning about viewpoint changes both at the level of places in a topological graph as well as fine-grained movements.

## VI. EXPERIMENTAL SETUP

We test the following hypotheses through our experiments:

- (1) Leveraging correlational information with easier-to-detect objects can benefit the search for hard-to-detect objects;
- (2) Optimizing over an action sequence improves performance compared to greedily choosing the next-best view.

### A. AI2-THOR

We conduct experiments in AI2-THOR [16], a realistic simulator of in-household rooms. It has a total of 120 scenes divided evenly into four room types: *Bathroom*, *Bedroom*, *Kitchen*, and *Living room*. For each room type, we use the first 20 scenes for training a vision-based object detector and learning object correlation models (used in some experiments), and the last 10 for evaluating performance.

The robot can take primitive move actions from the set:  $\{\text{MoveAhead}, \text{RotateLeft}, \text{RotateRight}, \text{LookUp}, \text{LookDown}\}$ . MoveAhead moves the robot forward by 0.25m. RotateLeft, RotateRight rotate the robot in place by 45°. LookUp, LookDown tilt the camera up or down by 30°. The transition function of the robot's viewpoint when taking primitive move actions is deterministic. All methods (Sec VI-G) receive observations of the robot's viewpoint without noise, that is  $O_{\text{robot}}(z_{\text{robot}}, s_{\text{robot}}) = \mathbb{1}(z_{\text{robot}} = s_{\text{robot}})$ . To be successful, when the robot takes Done, the robot must be within a Euclidean distance of 1.0m from the target object while the target object is visible in the camera frame. The maximum number of steps  $T_{\text{max}}$  is 100.

### B. Object Detector

Unlike previous work in object search evaluated using a ground truth object detector [21] or detectors with synthetic

noise and detection ranges [2], we use a vision-based object detector, YOLOv5 [18], since it is more realistic and suitable for our motivation. We collect training data by randomly placing the agent in the training scenes. Table II and Table III contain detection statistics of the target objects and correlated objects in validation scenes, respectively. The pixel coordinates within the bounding boxes returned by YOLOv5 are downsampled and inverse projected to positions in the 3D world frame, using the provided depth image.

**Detection Model.** Vision detectors can sometimes detect small objects from far away. Therefore, we consider a line-of-sight detection model with a limited field of view angle to enable POMDP planning:

$$D(z_i, x_i, s_{\text{robot}}) = \Pr(z_i | x_i, s_{\text{robot}}) = \begin{cases} 1.0 - \text{TP} & s_i \in \mathcal{V}(s_{\text{robot}}) \wedge z_i = \text{null} \\ \delta \text{FP} / |\mathcal{V}_E(r)| & s_i \in \mathcal{V}(s_{\text{robot}}) \wedge \|z_i - x_i\| > 3\sigma \\ \delta \mathcal{N}(z_i; x_i, \sigma^2) & s_i \in \mathcal{V}(s_{\text{robot}}) \wedge \|z_i - x_i\| \leq 3\sigma \\ 1.0 - \text{FP} & s_i \notin \mathcal{V}(s_{\text{robot}}) \wedge z_i = \text{null} \\ \delta \text{FP} / |\mathcal{V}_E(r)| & s_i \notin \mathcal{V}(s_{\text{robot}}) \wedge z_i \neq \text{null} \end{cases}$$

This detection model is parameterized by: TP, the true positive rate; FP, the false positive rate;  $r$ , the average distance between the robot and the object for true positive detections;  $\sigma$ , the width of a small region around the true object location where a detection made within that region, though not exactly accurate, is still accepted as a true positive detection. We set  $\sigma = 0.5\text{m}$ . The notation  $\mathcal{N}(\cdot; x_i, \sigma^2)$  denotes a Gaussian distribution with mean  $x_i$  and covariance  $\sigma^2 \mathbf{I}$ . The  $\mathcal{V}(s_{\text{robot}})$  denotes the line-of-sight field of view with a  $90^\circ$  angle. The  $\mathcal{V}_E(r)$  denotes the region inside the field of view that is within distance  $r$  from the robot. The weight  $\delta = 1$  if the detection is within  $\mathcal{V}_E(r)$ , and otherwise  $\delta = \exp(-\|z_i - s_{\text{robot}}\| - r)^2$ .

### C. Target Objects

The list of target object classes and other correlated classes for each room type is listed below (with no particular order). For detection statistics, please refer to Table I and Table III (Appendix C).

- *Bathroom* - Targets: Faucet, Candle, ScrubBrush; Correlated objects: ToiletPaperHanger, Towel, Mirror, Toilet, SoapBar.
- *Bedroom* - Targets: AlarmClock, Pillow, CD; Correlated objects: Laptop, DeskLamp, Mirror, LightSwitch, Bed.
- *Kitchen* - Targets are Bowl, Knife, PepperShaker; Correlated classes are: Lettuce, LightSwitch, Microwave, Plate, StoveKnob
- *Living room* - Targets are CreditCard, RemoteControl, Television; Correlated classes are: LightSwitch, Pillow, HousePlant, Laptop, FloorLamp, Painting.

### D. Correlation Model

We consider a binary correlation model that takes into account whether the correlated object and the target are close

or far. Specifically, we define:

$$C(x_{\text{target}}, x_i) = \Pr(x_i | x_{\text{target}}) \quad (7)$$

$$= \begin{cases} 1 & \text{Close}(i, \text{target}) \wedge \|x_i - x_{\text{target}}\| < d(i, \text{target}) \\ 0 & \text{Close}(i, \text{target}) \wedge \|x_i - x_{\text{target}}\| \geq d(i, \text{target}) \\ 1 & \text{Far}(i, \text{target}) \wedge \|x_i - x_{\text{target}}\| > d(i, \text{target}) \\ 0 & \text{Far}(i, \text{target}) \wedge \|x_i - x_{\text{target}}\| \leq d(i, \text{target}) \end{cases} \quad (8)$$

where  $\text{Close}(\cdot, \cdot)$  and  $\text{Far}(\cdot, \cdot)$  are class-level predicates,  $\|\cdot\|$  denotes the Euclidean distance, and  $d(\cdot, \cdot)$  is the expected distance between the two objects. This model is applicable between arbitrary object classes and can be estimated based on instances of object classes. In Sec. VII-A, we conduct an ablation study where  $d(\cdot, \text{target})$  is estimated under different scenarios: **accurate**: based on object ground truth locations in the deployed scene; **learned** (lrn): based on instances in training scenes; **wrong** (wrg): same as accurate except we flip the close/far relationship between the objects so that they do not match the scene.

### E. Implementation Detail of COS-POMDP

Objects exist in 3D space in AI2-THOR scenes, and the robot can rotate its camera both horizontally and vertically. Our implementation of COS-POMDP allows for search in such a setting by estimating, in the belief over target locations, both the 2D position of the target as well as the height of the target. Since the robot can tilt only its camera within a small range of angles, we consider a discrete set of possible height values, Above, Below, and Same, which indicates the object is above, below, or at the same level with respect to the camera's current tilt angle. Our implementation is based on the pomdp\_py [42] library.

### F. Evaluation Metric

We use three metrics: (1) success weighted by inverse path length (SPL) [19]; (2) success rate (SR) and (3) discounted cumulative rewards (DR). The SPL of each search trial is defined as  $SPL = S \cdot \ell / \max(p, \ell)$  where  $S$  is the binary success outcome of the search,  $\ell$  is the shortest path between the robot and the target, and  $p$  is the actual search path. The SPL measures the search performance by taking into account both the success and efficiency of the search. It is a difficult metric because  $\ell$  uses information about the true object location. However, it does not penalize excessive rotations [22]. Therefore, we also include discounted cumulative rewards ( $\gamma = 0.95$ ) which takes such actions into account.

### G. Baselines

Baselines are defined in the caption of Table I. Note that for **Greedy-NBV**, based on [2], a weighted particle belief is used to maintain the belief over the joint state over all object locations. During planning, the agent selects the next best viewpoint to navigate towards based on a cost function that considers both navigation distance and the probability of detecting any object. This provides a baseline that is in contrast to the sequential decision-making paradigm considered by COS-POMDPs and the modeling of only robot and target states.

Method	Bathroom			Bedroom			Kitchen			Living room		
	SPL (%)	DR	SR (%)	SPL (%)	DR	SR (%)	SPL (%)	DR	SR (%)	SPL (%)	DR	SR (%)
Random	0.00 (0.00)	-82.75 (3.43)	0.00	0.00 (0.00)	-85.27 (3.82)	0.00	6.90 (9.81)	-68.51 (15.61)	6.90	0.00 (0.00)	-82.37 (3.62)	0.00
Greedy-NBV	14.85 (9.40)	-18.86 (12.14)	35.71	<b>31.10 (17.86)</b>	<b>-6.97 (14.20)</b>	<b>40.91</b>	12.03 (9.01)	-17.16 (12.85)	32.14	7.13 (7.11)	-21.41 (8.21)	20.00
Target-POMDP	24.17 (12.03)	<b>-2.60 (17.02)</b>	<b>66.67</b>	14.70 (12.86)	-26.74 (13.27)	31.58	14.82 (9.22)	-20.06 (13.85)	37.04	<b>29.23 (15.34)</b>	-30.65 (13.60)	48.00
COS-POMDP	<b>30.03 (13.59)</b>	-14.92 (12.76)	56.00	28.54 (17.63)	-16.02 (14.03)	40.00	<b>20.95 (13.10)</b>	<b>-4.67 (14.71)</b>	<b>44.00</b>	27.76 (15.21)	<b>-12.32 (15.71)</b>	<b>48.15</b>
COS-POMDP (gt)	<b>33.38 (13.92)</b>	-11.69 (13.24)	62.96	<b>39.22 (19.56)</b>	-13.50 (17.28)	<b>56.25</b>	<b>36.92 (14.33)</b>	<b>-2.92 (16.46)</b>	<b>64.00</b>	<b>35.71 (16.05)</b>	<b>-9.31 (13.09)</b>	<b>62.50</b>
COS-POMDP (lrn)	19.77 (12.07)	-21.53 (13.13)	45.83	16.43 (14.53)	-33.73 (11.05)	23.81	6.29 (6.93)	-32.72 (13.62)	17.86	14.76 (11.41)	-43.09 (13.57)	25.00
COS-POMDP (wrg)	10.83 (7.79)	-19.00 (10.21)	28.00	14.54 (14.29)	-32.54 (14.87)	27.78	8.80 (7.38)	-20.49 (10.63)	25.93	<b>29.34 (16.10)</b>	-16.15 (11.96)	<b>54.17</b>

TABLE I: **Main and Ablation Study Results.** Unless otherwise specified, all methods use the YOLOv5 [18] vision detector and are given accurate correlational information. **Target-POMDP** uses the hierarchical planning except only the target object is detectable. **Greedy-NBV** is a next-best view approach based on [2]. **Random** chooses actions uniformly at random. The highest value of each metric per room type is bolded. Parentheses contain 95% confidence interval. Ablation study results are bolded if it outperforms the best result from the main evaluation. Metrics are success weighted by inverse path length (SPL) [19], discounted cumulative reward (DR), and success rate (SR). **COS-POMDP** is more consistent, performing either the best or the second best across all room types and metrics.

Room Type	Target Class	Greedy-NBV			Target-POMDP			COS-POMDP		
		TP	FP	$r$ (m)	SPL (%)	DR	SR (%)	SPL (%)	DR	SR (%)
Bathroom	Faucet	56.1	8.0	2.16	31.45 (20.79)	6.11 (21.02)	<b>77.78</b>	<b>40.21 (27.65)</b>	<b>13.97 (30.40)</b>	75.00
	Candle	29.4	2.4	1.81	12.52 (20.12)	-22.81 (20.80)	22.22	18.63 (14.51)	-6.61 (33.50)	<b>75.00</b>
	ScrubBrush	64.3	9.9	1.71	2.00 (4.52)	-37.79 (17.36)	10.00	7.38 (13.80)	-22.68 (34.63)	40.00
Bedroom	AlarmClock	79.6	7.4	2.77	<b>48.10 (43.23)</b>	<b>-0.80 (26.52)</b>	<b>57.14</b>	14.64 (46.61)	-17.37 (44.62)	25.00
	Pillow	88.3	5.2	2.43	<b>30.04 (49.28)</b>	<b>-13.59 (38.13)</b>	33.33	5.16 (14.32)	-29.49 (30.07)	<b>40.00</b>
	CD	48.6	4.5	1.70	18.59 (21.89)	<b>-7.36 (26.46)</b>	33.33	19.49 (22.66)	-29.12 (21.97)	30.00
Kitchen	Bowl	60.6	11.5	1.75	<b>19.88 (26.57)</b>	-15.76 (32.76)	33.33	16.33 (16.00)	-10.06 (27.39)	<b>55.56</b>
	Knife	37.7	8.7	1.68	8.22 (12.85)	-17.74 (26.85)	33.33	5.13 (11.84)	-37.99 (17.17)	11.11
	PepperShaker	38.1	9.4	1.43	8.39 (10.53)	-17.90 (17.39)	30.00	<b>22.99 (23.22)</b>	-12.14 (31.40)	<b>44.44</b>
Living room	Television	85.3	5.2	2.59	8.98 (18.36)	-22.86 (13.31)	20.00	<b>59.56 (25.42)</b>	<b>-6.50 (19.73)</b>	<b>88.89</b>
	RemoteControl	69.6	4.5	1.93	9.24 (13.99)	-13.21 (20.44)	30.00	26.67 (35.38)	-29.18 (20.47)	42.86
	CreditCard	42.9	4.3	1.48	3.18 (7.19)	<b>-28.15 (11.70)</b>	10.00	0.91 (2.09)	-55.95 (22.44)	11.11

TABLE II: **Detection Statistics and Object Search Results Grouped by Target Classes.** TP: true positive rate (%); FP: false positive rate (%);  $r$ : average distance to the true positive detections (m). We estimated these values by running the vision detector at 30 random camera poses per validation scene. Target objects are sorted by average detection range. Parentheses contain 95% confidence interval. Metrics are success weighted by inverse path length (SPL) [19], discounted cumulative reward (DR), and success rate (SR). **COS-POMDP** performs more robustly for hard-to-detect objects, such as ScrubBrush, CD, Candle, Knife, and CreditCard.

## VII. RESULTS AND DISCUSSIONS

Our main results are shown in Table I. The performance of **COS-POMDP** is the most consistent compared to other baselines, with **COS-POMDP** performing either the best or the second best in the four room types. The performance is broken down by target classes in Table II. **Greedy-NBV** performs well in *Bedroom*; it appears to experience less inaccuracy in the particle-based belief over all objects as a result of particle reinvigoration in bedroom compared to the other room types. **COS-POMDP** appears to be the most robust when the target object has significant noise of being correctly detected, including ScrubBrush, CreditCard, Candle RemoteControl, Knife, and CD. An example search trial of **COS-POMDP** for CreditCard is shown in Fig 3 and the search paths of the methods under comparison are visualized in Fig 4. For target objects with a true positive detection rate below 40%, **COS-POMDP** improves the POMDP baseline that ignores correlational information by 70% in terms of the SPL metric, and is more than 1.7 times better than the greedy baseline. Indeed, when the target object is reliably detectable, such as Television, the ability to detect multiple other objects may actually hurt performance, compared to **Target-POMDP**, due to the noise from detecting those other objects and the influence on search behavior. These results demonstrate that COS-POMDPs can be applied to search for hard-to-detect objects leveraging the more reliable detection of correlated objects.

### A. Ablation Studies

We also conduct two ablation studies. First, we equip **COS-POMDP** with a groundtruth object detector, as done in [21], henceforth called **COS-POMDP (gt)**. This shows the performance when the detections of both the target and correlated objects involve no noise at all. We observe better or competitive performance from using groundtruth detectors across all metrics in all room types.

Additionally, we use correlations obtained by learning from data (**COS-POMDP (lrn)**) as well as incorrect correlation information that is the reverse of the correct one (**COS-POMDP (wrg)**). Indeed, using accurate correlations provides the most benefit, while correlations learned through this simple method could offer benefit compared to using incorrect correlations in some cases (*Bathroom* and *Bedroom*), but can also backfire and hurt performance in other others. Therefore, properly learning correlation is important, while leveraging a reliable source of information, for example, from a human at the scene, may offer the most benefit.

## VIII. CONCLUSIONS

In this paper, we formulated the problem of correlational object search and proposed COS-POMDP, a POMDP-based approach to model this problem. Our quantitative evaluation, conducted in AI2-THOR [16] using the YOLOv5 [17, 18] detector, demonstrates the benefit of our approach in exploiting the correlational information with easier-to-detect objects



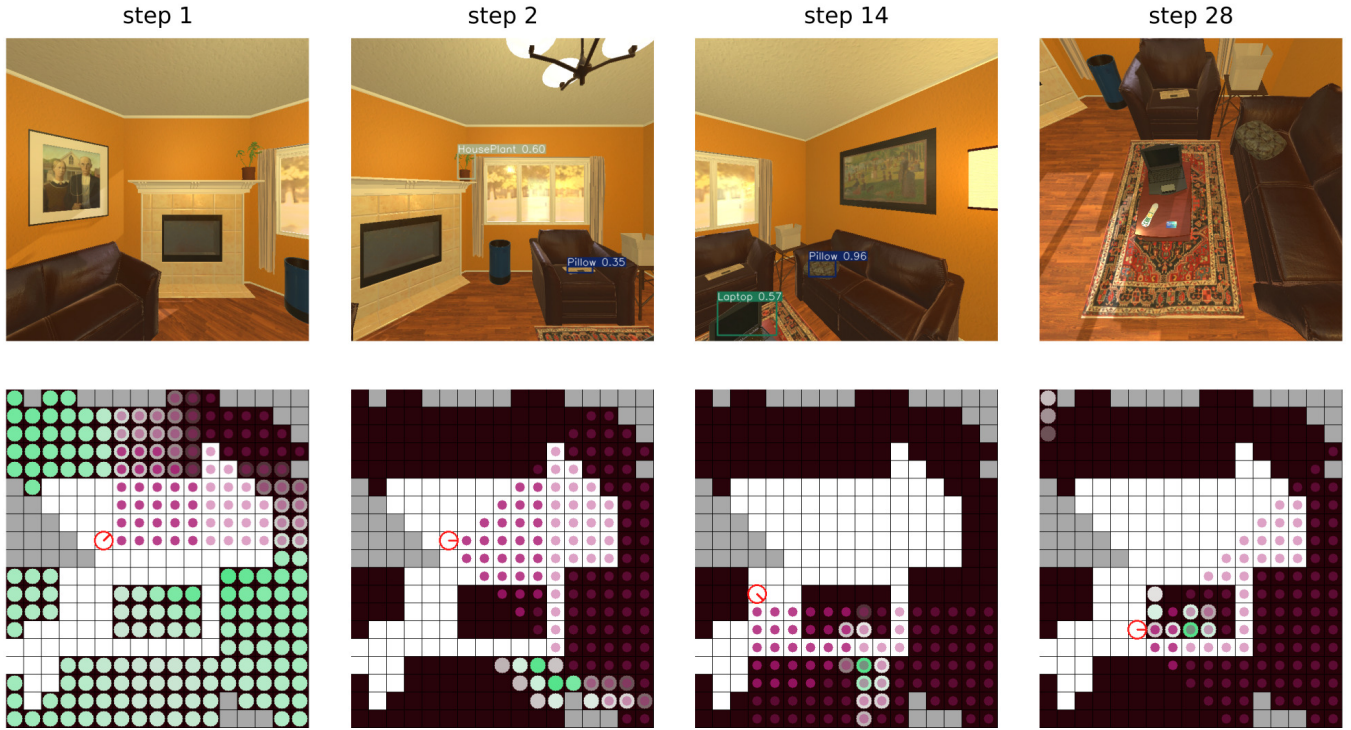


Fig. 3: **Example Sequence.** Top: first-person view with object detection bounding boxes. Bottom: Visualization of belief state corresponding to each view. See Fig 2 for the legend of the belief state visualization. Our method (COS-POMDP) successfully finds a CreditCard in a living room scene, leveraging the detection of other objects such as FloorLamp and Laptop. For more examples, please refer to the video at <https://youtu.be/wd1tmD0mckY>.



Fig. 4: Visualization of robot trajectory produced by different methods for the example shown in Fig. 3. Each gray circle represents the position of a viewpoint, and each black line segment indicates the orientation of the robot’s camera at a viewpoint. The path traversed during the search is shown in blue.

to find hard-to-detect objects. Future work directions include studying the search behavior given different kinds of learned correlation models as well as in more complex settings that involve *e.g.*, container opening and dynamic objects.

#### ACKNOWLEDGEMENTS

We sincerely thank Leslie Kaelbling and Tomás Lozano-Pérez for their critical and invaluable advice. We also thank Mitchell Wortsman, Yiding Qiu, and Anwesan Pal for clarifications about their works, as well as Matt Deitke and the AI2-THOR developers for patiently answering our questions about AI2-THOR. This work was supported by the National Science Foundation under grant number IIS1652561, the US Army under grant number W911NF1920145, and the Office of Naval Research under the PERISCOPE MURI Contract N00014-17-1-2699.

#### REFERENCES

- [1] D. Sprute, A. Pörtner, R. Rasch, S. Battermann, and M. König, “Ambient assisted robot object search,” in *International Conference on Smart Homes and Health Telematics*. Springer, 2017.
- [2] Z. Zeng, A. Röfer, and O. C. Jenkins, “Semantic linking maps for active visual object search,” *IEEE*, 2020, pp. 1984–1990.
- [3] M. T. Eismann, A. D. Stocker, and N. M. Nasrabadi, “Automated hyperspectral cueing for civilian search and rescue,” *Proceedings of the IEEE*, vol. 97, no. 6, pp. 1031–1055, 2009.
- [4] J. Sun, B. Li, Y. Jiang, and C.-y. Wen, “A camera-based target detection and positioning uav system for search and rescue (SAR) purposes,” *Sensors*, vol. 16, no. 11, p. 1778, 2016.
- [5] I. Idrees, S. P. Reiss, and S. Tellex, “Robomem: Giving long term memory to robots,” *arXiv preprint arXiv:2003.10553*, 2020.
- [6] M. R. Loghmani, T. Patten, and M. Vincze, “Towards socially assistive robots for elderly: An end-to-end object search framework,” in *2018 IEEE International Conference on Pervasive Computing and Communications Workshops (PerCom Workshops)*. IEEE, 2018.
- [7] A. Aydemir, A. Pronobis, M. Göbelbecker, and P. Jensfelt, “Active visual object search in unknown environments using uncertain semantics,” *IEEE Transactions on Robotics*, vol. 29, no. 4, pp. 986–1002, 2013.
- [8] T. Kollar and N. Roy, “Utilizing object-object and object-scene context when planning to find things,” in *2009 IEEE International Conference on Robotics and Automation*. IEEE, 2009, pp. 2168–2173.
- [9] J. K. Li, D. Hsu, and W. S. Lee, “Act to see and see to act: POMDP planning for objects search in clutter,” in *2016 IEEE/RSJ International Conference on Intelligent Robots and Systems (IROS)*. IEEE, 2016.
- [10] Y. Xiao, S. Katt, A. ten Pas, S. Chen, and C. Amato, “Online planning for target object search in clutter under partial observability,” in *Proceedings of the International Conference on Robotics and Automation*, 2019.
- [11] A. Wandzel, Y. Oh, M. Fishman, N. Kumar, and S. Tellex, “Multi-object search using object-oriented POMDPs,” in *2019 International Conference on Robotics and Automation (ICRA)*. IEEE, 2019.
- [12] K. Zheng, Y. Sung, G. Konidaris, and S. Tellex, “Multi-resolution



POMDP planning for multi-object search in 3D,” in *IEEE/RSJ International Conference on Intelligent Robots and Systems (IROS)*, 2021.

[13] R. Krishna, Y. Zhu, O. Groth, J. Johnson, K. Hata, J. Kravitz, S. Chen, Y. Kalantidis, L.-J. Li, D. A. Shamma *et al.*, “Visual genome: Connecting language and vision using crowdsourced dense image annotations,” *International journal of computer vision*, vol. 123, no. 1, pp. 32–73, 2017.

[14] T. Kollar, S. Tellex, D. Roy, and N. Roy, “Toward understanding natural language directions,” in *2010 5th ACM/IEEE International Conference on Human-Robot Interaction (HRI)*. IEEE, 2010.

[15] K. Zheng, D. Bayazit, R. Mathew, E. Pavlick, and S. Tellex, “Spatial language understanding for object search in partially observed cityscale environments,” in *International Conference on Robot and Human Interactive Communication (RO-MAN)*. IEEE, 2021.

[16] E. Kolve, R. Mottaghi, W. Han, E. VanderBilt, L. Weihs, A. Herrasti, D. Gordon, Y. Zhu, A. Gupta, and A. Farhadi, “Ai2-thor: An interactive 3d environment for visual ai,” *arXiv preprint arXiv:1712.05474*, 2017.

[17] J. Redmon, S. Divvala, R. Girshick, and A. Farhadi, “You only look once: Unified, real-time object detection,” in *Proceedings of the IEEE conference on computer vision and pattern recognition*, 2016.

[18] G. Jocher, A. Stoken, J. Borovec, NanoCode012, ChristopherSTAN, L. Changyu, Laughing, tkianai, A. Hogan, lorenzomammanna, yxNONG, AlexWang1900, L. Diaconu, Marc, wanghaoyang0106, ml5ah, Doug, F. Ingham, Frederik, Guilhen, Hatovix, J. Poznanski, J. Fang, L. Yu, changyu98, M. Wang, N. Gupta, O. Akhtar, PetrDvoracek, and P. Rai, “ultralytics/yolov5: v3.1 - Bug Fixes and Performance Improvements,” Oct. 2020. [Online]. Available: <https://doi.org/10.5281/zenodo.4154370>

[19] P. Anderson, A. Chang, D. S. Chaplot, A. Dosovitskiy, S. Gupta, V. Koltun, J. Kosecka, J. Malik, R. Mottaghi, M. Savva *et al.*, “On evaluation of embodied navigation agents,” *arXiv preprint arXiv:1807.06757*, 2018.

[20] M. Wortsman, K. Ehsani, M. Rastegari, A. Farhadi, and R. Mottaghi, “Learning to learn how to learn: Self-adaptive visual navigation using meta-learning,” in *The IEEE Conference on Computer Vision and Pattern Recognition (CVPR)*, June 2019.

[21] Y. Qiu, A. Pal, and H. I. Christensen, “Learning hierarchical relationships for object-goal navigation,” in *2020 Conference on Robot Learning (CoRL)*, 2020.

[22] D. Batra, A. Gokaslan, A. Kembhavi, O. Maksymets, R. Mottaghi, M. Savva, A. Toshev, and E. Wijmans, “Objectnav revisited: On evaluation of embodied agents navigating to objects,” *arXiv preprint arXiv:2006.13171*, 2020.

[23] Y. Ye and J. K. Tsotsos, “Sensor planning in 3d object search: its formulation and complexity,” in *The 4th International Symposium on Artificial Intelligence and Mathematics, Florida, USA*. Citeseer, 1996.

[24] L. L. Wong, L. P. Kaelbling, and T. Lozano-Pérez, “Manipulation-based active search for occluded objects,” in *2013 IEEE International Conference on Robotics and Automation*. IEEE, 2013, pp. 2814–2819.

[25] T. Novkovic, R. Pautrat, F. Furrer, M. Breyer, R. Siegwart, and J. Nieto, “Object finding in cluttered scenes using interactive perception,” in *2020 IEEE International Conference on Robotics and Automation (ICRA)*. IEEE, 2020, pp. 8338–8344.

[26] S. S. Brown, “Optimal search for a moving target in discrete time and space,” *Operations research*, vol. 28, no. 6, pp. 1275–1289, 1980.

[27] C. Wang, J. Cheng, J. Wang, X. Li, and M. Q.-H. Meng, “Efficient object search with belief road map using mobile robot,” *IEEE Robotics and Automation Letters*, vol. 3, no. 4, pp. 3081–3088, 2018.

[28] M. Lorbach, S. Höfer, and O. Brock, “Prior-assisted propagation of spatial information for object search,” in *2014 IEEE/RSJ International Conference on Intelligent Robots and Systems*. IEEE, 2014.

[29] Y. Zhang, G. Tian, J. Lu, M. Zhang, and S. Zhang, “Efficient dynamic object search in home environment by mobile robot: A priori knowledge-based approach,” *IEEE Transactions on Vehicular Technology*, vol. 68, no. 10, pp. 9466–9477, 2019.

[30] L. Kunze, K. K. Doreswamy, and N. Hawes, “Using qualitative spatial relations for indirect object search,” in *2014 IEEE international conference on robotics and automation (ICRA)*. IEEE, 2014.

[31] T. D. Garvey, “Perceptual strategies for purposive vision,” *Thesis Ph.D. Stanford University*, 1976.

[32] L. E. Wixson and D. H. Ballard, “Using intermediate objects to improve the efficiency of visual search,” *International Journal of Computer Vision*, vol. 12, no. 2-3, pp. 209–230, 1994.

[33] Y. Zhu, R. Mottaghi, E. Kolve, J. J. Lim, A. Gupta, L. Fei-Fei, and A. Farhadi, “Target-driven visual navigation in indoor scenes using

deep reinforcement learning,” in *2017 IEEE international conference on robotics and automation (ICRA)*. IEEE, 2017, pp. 3357–3364.

- [34] B. Mayo, T. Hazan, and A. Tal, “Visual navigation with spatial attention,” in *Proceedings of the IEEE/CVF Conference on Computer Vision and Pattern Recognition*, 2021, pp. 16898–16907.
- [35] L. P. Kaelbling, M. L. Littman, and A. R. Cassandra, “Planning and acting in partially observable stochastic domains,” *Artificial intelligence*, vol. 101, no. 1-2, pp. 99–134, 1998.
- [36] G. Shani, J. Pineau, and R. Kaplow, “A survey of point-based POMDP solvers,” *Autonomous Agents and Multi-Agent Systems*, 2013.
- [37] A. Somani, N. Ye, D. Hsu, and W. S. Lee, “Despot: Online POMDP planning with regularization,” in *NIPS*, vol. 13, 2013, pp. 1772–1780.
- [38] D. Silver and J. Veness, “Monte-carlo planning in large POMDPs,” in *Neural Information Processing Systems*, 2010.
- [39] K. Zheng, “ROS Navigation Tuning Guide,” in *Robot Operating System (ROS)*, A. Koubaa, Ed. Springer International Publishing, 2021, ch. 6, pp. 197–226.
- [40] S. Macenski, F. Martín, R. White, and J. G. Clavero, “The marathon 2: A navigation system,” in *2020 IEEE/RSJ International Conference on Intelligent Robots and Systems (IROS)*. IEEE, 2020, pp. 2718–2725.
- [41] K. Zheng and A. Pronobis, “From pixels to buildings: End-to-end probabilistic deep networks for large-scale semantic mapping,” in *2019 IEEE/RSJ International Conference on Intelligent Robots and Systems (IROS)*, 2019, pp. 3511–3518.
- [42] K. Zheng and S. Tellex, “pomdp\_py: A framework to build and solve POMDP problems,” in *ICAPS 2020 Workshop on Planning and Robotics (PlanRob)*, 2020.

## APPENDIX

### A. Proof of Theorem 1

**Theorem 1.** Given any policy  $\pi : h_t \rightarrow a$ , the distribution of histories is identical between the COS-POMDP and the F-POMDP.

*Proof:* We prove this by induction. When  $t = 1$ , the statement is true because both histories are empty. The inductive hypothesis assumes that the distributions  $\Pr(h_t)$  is the same for the two POMDPs at  $t \geq 1$ . Then, by definition,  $\Pr(h_{t+1}) = \Pr(h_t, a_t, z_t) = \Pr(z_t|h_t, a_t) \Pr(a_t|h_t) \Pr(h_t)$ . Since  $\Pr(a_t|h_t)$  is the same under the given  $\pi$ , we can conclude  $\Pr(h_{t+1})$  is identical if the two POMDPs have the same  $\Pr(z_t|h_t, a_t)$ . We show that this is true as follows.

First, we sum out the state  $s_t$  at time  $t$ :

$$\Pr(z_t|h_t, a_t) = \sum_{s_t} \Pr(s_t, z_t|h_t, a_t) \quad (9)$$

By definition of conditional probability,

$$= \sum_{s_t} \Pr(z_t|s_t, h_t, a_t) \Pr(s_t|h_t, a_t) \quad (10)$$

Since  $s_t$  is does not depend on  $a_t$  (which affects  $s_{t+1}$ ),

$$= \sum_{s_t} \Pr(z_t|s_t, h_t, a_t) \Pr(s_t|h_t) \quad (11)$$

Suppose we are deriving this distribution for COS-POMDP, denoted as  $\Pr_{\text{COS-POMDP}}(z_t|h_t, a_t)$ . Then, by definition, the state  $s_t = (x_{\text{target}}, s_{\text{robot}})$ . Therefore, we can write:

$$\begin{aligned} & \Pr_{\text{COS-POMDP}}(z_t|h_t, a_t) \\ &= \sum_{x_{\text{target}}, s_{\text{robot}}} \Pr(z_t|x_{\text{target}}, s_{\text{robot}}, h_t, a_t) \\ & \quad \times \Pr(x_{\text{target}}, s_{\text{robot}}|h_t) \end{aligned} \quad (12)$$

Summing out  $x_1, \dots, x_n$ ,

$$= \sum_{x_{\text{target}}, s_{\text{robot}}} \sum_{x_1, \dots, x_n} \Pr(x_1, \dots, x_n, z_t | x_{\text{target}}, s_{\text{robot}}, h_t, a_t) \times \Pr(x_{\text{target}}, s_{\text{robot}} | h_t) \quad (13)$$

Merging sum,

$$= \sum_{\substack{x_1, \dots, x_n, \\ x_{\text{target}}, s_{\text{robot}}}} \Pr(x_1, \dots, x_n, z_t | x_{\text{target}}, s_{\text{robot}}, h_t, a_t) \times \Pr(x_{\text{target}}, s_{\text{robot}} | h_t) \quad (14)$$

By the definition of conditional probability,

$$= \sum_{\substack{x_1, \dots, x_n, \\ x_{\text{target}}, s_{\text{robot}}}} \Pr(z_t | x_1, \dots, x_n, x_{\text{target}}, s_{\text{robot}}, h_t, a_t) \times \Pr(x_1, \dots, x_n | x_{\text{target}}, s_{\text{robot}}, h_t, a_t) \times \Pr(x_{\text{target}}, s_{\text{robot}} | h_t) \quad (15)$$

Again, because the object locations are independent of  $a_t$ ,

$$= \sum_{\substack{x_1, \dots, x_n, \\ x_{\text{target}}, s_{\text{robot}}}} \Pr(z_t | x_1, \dots, x_n, x_{\text{target}}, s_{\text{robot}}, h_t, a_t) \times \Pr(x_1, \dots, x_n | x_{\text{target}}, s_{\text{robot}}, h_t) \times \Pr(x_{\text{target}}, s_{\text{robot}} | h_t) \quad (16)$$

By the definition of conditional probability again,

$$= \sum_{\substack{x_1, \dots, x_n, \\ x_{\text{target}}, s_{\text{robot}}}} \Pr(z_t | x_1, \dots, x_n, x_{\text{target}}, s_{\text{robot}}, h_t, a_t) \times \Pr(x_1, \dots, x_n, x_{\text{target}}, s_{\text{robot}} | h_t) \quad (17)$$

Note that  $(x_{\text{target}}, s_{\text{robot}}, x_1, \dots, x_n)$  is a state in F-POMDP. Denote the state space of F-POMDP as  $\mathcal{S}_F$ . According to Eq (11), we can write the above Eq (17) as

$$= \sum_{s_t \in \mathcal{S}_F} \Pr(z_t | s_t, h_t, a_t) \Pr(s_t | h_t) \quad (18)$$

$$= \Pr_{\text{F-POMDP}}(z_t | h_t, a_t) \quad (19)$$

### B. Auxiliary Procedures

Algorithm 2 is the pseudocode of the SampleTopoGraph algorithm, implemented for our experiments in AI2-THOR. We set  $M = 10$ ,  $d_{\text{sep}} = 1.0\text{m}$ ,  $\zeta_{\min} = 3$ ,  $\zeta_{\max} = 5$ . In our implementation, the topological graph is resampled only if the cumulative belief captured by the nodes in the current topological graph,  $\sum_{s_{\text{robot}} \in \mathcal{V}} p(s_{\text{robot}})$ , is below 50%. Otherwise, the same topological graph will be returned. Note that depending on the application domain, a different algorithm for forming the topological graph may be used in the place of SampleTopoGraph in the OnlineHierarchicalPlanning algorithm (Algorithm 1).

### Algorithm 2: SampleTopoGraph

---

**Input:**  $\mathcal{X}, \mathcal{S}_{\text{robot}}, b_{\text{target}}$   
**Parameter:** maximum number of nodes  $M$ , minimum separation between nodes  $d_{\text{sep}}$ , minimum and maximum out-degrees  $\zeta_{\min}, \zeta_{\max}$   
**Output:** A topological graph  $(\mathcal{V}, \mathcal{E})$   
 // Obtain mapping from  $s_{\text{robot}}$  to a set of closest locations  
**foreach**  $x \in \mathcal{X}$  **do**  
      $s_{\text{robot}}^{\text{closest}} \leftarrow \operatorname{argmin}_{s_r \in \mathcal{S}_{\text{robot}}} \|s_r.\text{pos} - x\|;$   
      $U(s_{\text{robot}}^{\text{closest}}) \leftarrow U(s_{\text{robot}}^{\text{closest}}) \cup \{x\};$   
**end**  
 // Construct probability distribution over  $\mathcal{S}_{\text{robot}}$  using  $b_{\text{target}}$   
**foreach**  $s_{\text{robot}} \in \mathcal{S}_{\text{robot}}$  **do**  
      $p(s_{\text{robot}}) \leftarrow \sum_{x \in U(s_{\text{robot}})} b_{\text{target}}(x)$   
**end**  
 // Construct nodes and edges  
 $\mathcal{V} \leftarrow \text{sample} \leq M$  nodes from  $\mathcal{S}_{\text{robot}}$  according to  $p$  such that any pair of nodes has a minimum distance of  $d_{\text{sep}}$ ;  
 $\mathcal{E} \leftarrow$  add edges between nodes in  $\mathcal{V}$  so that the graph is connected and each node has an out-degree between  $\zeta_{\min}$  and  $\zeta_{\max}$ ;  
**return**  $(\mathcal{V}, \mathcal{E})$

---

### C. Detection Statistics for Correlated Object Classes

Table III shows the detection statistics for correlated object classes. The detection statistics of target object classes can be found in Table II.

Room Type	Correlated Object Class	TP	FP	$r$ (m)
Bathroom	Mirror	76.9	3.7	2.10
	ToiletPaperHanger	84.4	1.5	1.96
	Towel	79.4	2.7	1.88
	Toilet	86.3	3.5	1.81
	SoapBar	73.2	1.8	1.53
Bedroom	DeskLamp	89.5	2.6	2.41
	Bed	63.5	0.6	2.39
	Mirror	86.0	0.6	2.27
	LightSwitch	76.3	2.8	2.26
	Laptop	75.9	1.2	2.19
Kitchen	LightSwitch	90.0	3.9	2.57
	Microwave	75.3	5.6	2.31
	StoveKnob	82.8	5.6	2.00
	Lettuce	98.6	0.3	1.98
	Plate	60.6	3.2	1.90
Living room	FloorLamp	71.7	5.1	3.44
	Painting	85.2	4.0	3.18
	LightSwitch	80.6	1.5	3.10
	HousePlant	82.9	3.9	3.00
	Pillow	67.4	2.8	2.84
	Laptop	66.3	2.6	2.24

TABLE III: Detection Statistics for Correlated Object Classes. TP: true positive rate (%); FP: false positive rate (%);  $r$ : average distance to the true positive detections (m). We estimated these values by running the vision detector at 30 random camera poses per validation scene. The correlated object classes for each room type are sorted by average detection range.